Water Conservation and Management (WCM)

DOI: http://doi.org/10.26480/wcm.01.2026.220.229

ISSN: 2523-5664 (Print)
ISSN: 2523-5672 (Online)
CODEN: WCMABD

RESEARCH ARTICLE

EXPERIMENTAL EVALUATION OF SILL CONFIGURATIONS IN STILLING BASINS FOR EFFICIENT ENERGY DISSIPATION IN HYDRAULIC STRUCTURES

Very Dermawan[a*], Sandi Erryanto[b], Evi Nur Cahya[a], Sumiadi[a]

[a]*Universitas Brawijaya, Department of Water Resources Engineering, Jalan MT Haryono, No. 167, Malang 65145, East Java, Indonesia*
[b]*Ministry of Public Work and Housing, Jalan Pattimura No. 20, Kebayoran Baru, Jakarta Selatan 12110, Indonesia*
**Corresponding Author Email: peryderma@ub.ac.id*

Article History:

Received 27 January 2026
Revised 20 February 2026
Accepted 25 March 2026
Available online 12 May 2026

ABSTRACT

Improving energy dissipation and efficiency in hydraulic structures such as spillways, sluices, and weirs, is important to prevent downstream erosion and structural damage under high velocity (supercritical) flows. However, conventional stilling basin designs often fail to optimize hydraulic jump characteristics, particularly under strong hydraulic jump conditions. This study experimentally evaluates the hydraulic performance of single sill and double sill configurations of stilling basin in a laboratory-scale stilling basin under strong hydraulic jump conditions ($11<F_1<13.2$). A series of physical model experiments was conducted by varying sill geometry, height, and spacing. The results showed that the double sill configuration in Series DS-5, combination of an ogee sill (Z_1 = 6 cm) and a trapezoidal prism sill (Z_2 = 4.5 cm) spaced at L_1 = 80 cm, L_2 = $0.5L_1$ (40 cm), provides superior hydraulic performance compared to single sill and horizontal apron configurations. Series DS-5 achieved the lowest y_2 and y_j, the highest relative energy dissipation ($(E_0–E_2)/E_0$ = 81.42%), and average energy efficiency (E_2/E_1 = 51.31%). The enhanced performance is attributed to intensified turbulence interaction and improved hydraulic jump control induced by combined sill geometry. Regression based relationships between dimensionless hydraulic variables were also developed to support predictive design. This research contributes a practical and compact stilling basin design for high energy flow conditions, offering improved efficiency and potential application in hydraulic structure design.

KEYWORDS

Hydraulic jump, Stilling basin, Energy dissipation, Single ogee sill, Double sill, Hydraulic modeling, Froude number

1. INTRODUCTION

Hydraulic models are fundamental to the design and optimization of energy dissipation structures, particularly stilling basins, which transition supercritical flows into subcritical flows at downstream of hydraulic structures such as spillways and sluic es (Rabiei et al., 2023; Idfi et al., 2024; Al-Mansori et al., 2020; Kumcu and Ispir, 2022; Erryanto and Dermawan, 2024; Chanson, 2022; Al-Fatlawi et al., 2020). Effective stilling basin design is critical to dissipating energy and preventing erosion or structural failure (Raza et al., 2023; Nasiri et al., 2012; Zaffar et al., 2023). A persistent challenge lies in predicting hydraulic jump characteristics and achieving efficient dissipation within limited basin length (Fatimah et al., 2023; Liu et al., 2020; Hadi and Al-Qaisi, 2025; El-Saie et al., 2023). Geometric sill modification has proven effective in enhancing hydraulic performance by stabilizing jumps and influencing turbulence intensity and energy (Jiang et al., 2025; AlTalib et al., 2019; Al-Fatlawi et al., 2020; Hadi and Al-Qaisi, 2025; Mahmoud and Mohamed, 2022; Zaffar and Hassan, 2023) . Variation in sill height, shape, and position markedly affect sequent depth, jump length, and dissipation efficiency (Zhou et al., 2023; Mohammed Saleh and Khassaf, 2023; Tajabadi et al., 2018). The interaction between flow dynamics, sill-induced vortices, and basin geometry complicates the identification of optimal configurations. Recent studies have advanced sill-based design, though remain limited to simplified geometries, neglecting sustainability and adaptability (Zaffar and Hassan, 2023; Liu et al., 2020; Benabid et al., 2024). Numerical analyses have evaluated performance across configurations, but comprehensive assessment of combined sill types, such as ogee and trapezoidal prism forms, are scarce (Li et al., 2021; Roy et al., 2021; El-Saie et al., 2023; Roushangar and Homayounfar, 2019; Tan et al., 2025; Roy et al., 2021; Dharmadhikari and Gandhi, 2025; Kumar Jayant and Jhamnani, 2024). This gap highlights the potential of double sill systems, which may intensify turbulence, shorten jump, and mitigate scour (Erryanto and Dermawan, 2024; Saleh and Khassaf, 2024). However, the performance under high Froude numbers remains insufficiently validated.

This study introduces novel of single and double sill configurations, hypothesizing improved energy dissipation efficiency and reduced jump length. Laboratory scale experiments evaluate single and double sill configurations, quantifying energy loss and hydraulic jump. In addition, regression-based relationships between hydraulic variables and dimensionless parameters are developed to support predictive design. The findings of this research are expected to provide a practical framework for optimizing stilling basin design, particularly for compact, stable, and efficient energy dissipation systems in high-Froude number hydraulic structures ($11<F_1<13.2$).

Quick Response Code	Access this article online	
	Website: www.watconman.org	**DOI:** 10.26480/wcm.01.2026.220.229

Cite The Article: Very Dermawan, Sandi Erryanto, Evi Nur Cahya, Sumiadi (2026). Experimental Evaluation of Sill Configurations in Stilling Basins For Efficient Energy Dissipation in Hydraulic Structures. Water Conservation and Management, 10(1): 220-229.

2. Materials And Methods

The research was conducted at the River Engineering Laboratory, Universitas Brawijaya. The channel model had a width of 40 cm, wall height of 60 cm, spillway slope of 1:0.8 and height of 100 cm. The measurements carried out were flow depth (y_c, y_1, y_2), velocity (v_c, v_1, v_2), and the height and length of hydraulic jump (y_j, L_j) (Figure 1). The study was conducted using seven (7) flow rates: 15, 17, 19, 21, 23, 25, and 27 liters/second.

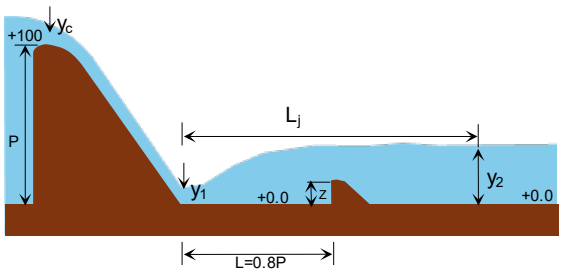

(i) Single ogee sill

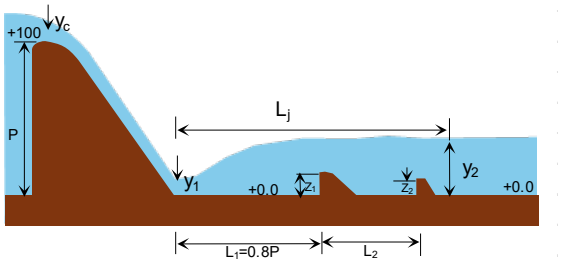

(ii) double sill (ogee and trapezoidal prism)

Figure 1: Hydraulic model in the laboratory and observed hydraulic parameters

Model calibration and verification are performed by comparing the analytical calculation results (expected) with the measurement on the model (observed). Analytical calculations are based on the law of flow continuity, the law of energy conservation, and the conjugation depth.

$$v = \frac{1}{n} R^{2/3} S^{1/2} \quad (1)$$

$$y_c = \sqrt[3]{\frac{Q^2}{B^2 g}} = \sqrt[3]{\frac{q^2}{g}} \quad (2)$$

$$F = \frac{v}{\sqrt{gy}} \quad (3)$$

$$\frac{y_2}{y_1} = \frac{1}{2}\sqrt{1 + 8F_1^2} - 1 \quad (4)$$

$$E = y + \frac{v^2}{2g} \quad (5)$$

$$MAPE = \frac{100\%}{n} \sum_{i=1}^{n} \left| \frac{y_i - \hat{y}_i}{y_i} \right| \quad (6)$$

Where: y_c = critical depth (m), Q = discharge (m^3/s), q= discharge per unit width (m^2/s), v = velocity (m/s), B = channel width (m), g = gravitational acceleration (m/s^2), E = flow energy (m), y = flow depth (m), MAPE = means absolute percentage error (%).

To strengthen the statistical interpretation of the experimental data, additional graphical analyses were included, such as hydraulic parameters regression plots and dimensionless hydraulic parameters relationships. These diagrams provide visual validation of the statistical correlation (R^2 values) and make the regression predictive model yielded in this study more intuitive. The plots presenting the data allow clearer identification of trends, data dispersion, and the reliability of the proposed equations.

The main hydraulic properties are spillway slope 1:0.8, n Manning=0.009. Froude number (F_1) in this case is $11 < F_1 < 13.2$ as shown in Table 1. The strong hydraulic jump was formed, $F_1 > 9$. By flowing the discharge according to y_c, the y_1 and y_2 are examined with high accuracy. Figure 2 shows an overview of part of calibration process to investigate y_1 and y_2.

Table 1: Analytical calculation of hydraulic parameters on the model

Q		B	q	y_c	$E_0 = E_c$	v_c	y_1	v_1	F_1	y_2	v_2	F_2
(L/s)	(m^3/s)	(m)	(m^2/s)	(m)	(m)	(m/s)	(m)	(m/s)		(m)	(m/s)	
15	0.015	0.4	0.0375	0.052	1.079	0.72	0.0094	3.99	13.14	0.1704	0.22	0.17
17	0.017	0.4	0.0425	0.057	1.085	0.75	0.0104	4.09	12.79	0.1830	0.23	0.17
19	0.019	0.4	0.0475	0.061	1.092	0.78	0.0114	4.17	12.46	0.1948	0.24	0.18
21	0.021	0.4	0.0525	0.065	1.098	0.8	0.0125	4.20	11.99	0.206	0.25	0.18
23	0.023	0.4	0.0575	0.07	1.104	0.83	0.0135	4.26	11.70	0.2166	0.27	0.18
25	0.025	0.4	0.0625	0.074	1.11	0.85	0.0146	4.28	11.31	0.2267	0.28	0.18
27	0.027	0.4	0.0675	0.077	1.115	0.87	0.0156	4.33	11.06	0.2364	0.29	0.19

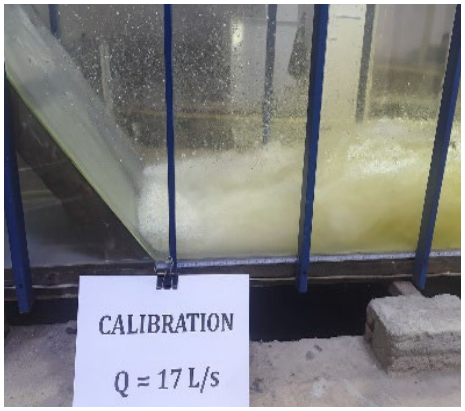

(a) Q=17 L/s

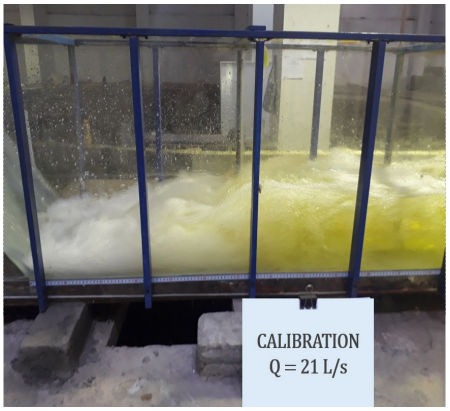

(b) Q=21 L/s

(c) Q=27 L/s

Figure 2: Initial hydraulic model running for investigations y_1 and y_2

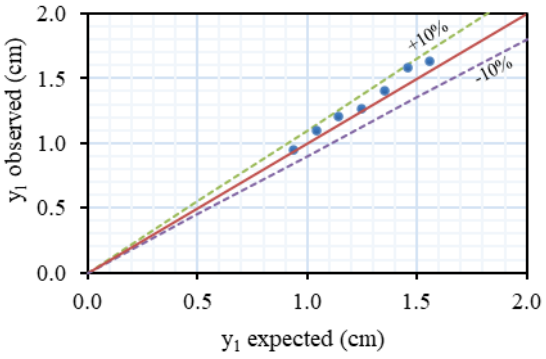

(a) Scatter plot of y_1 observed vs expected

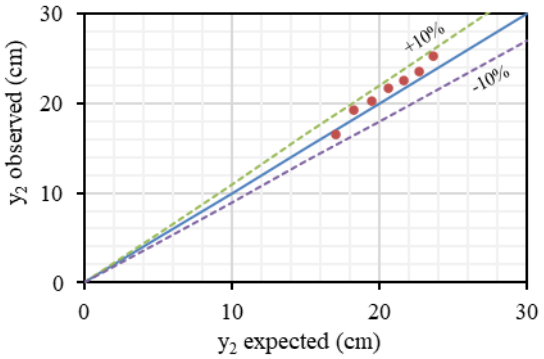

(b) Scatter plot y_2 observed vs expected

Figure 3: Comparison of y_1 and y_2 on model and analytical calculation

Figure 3 represents validation plots between observed and predicted values of y_1 and y_2, showing strong agreement with low deviation (MAPE<10%). It was found that MAPE y_1 = 4.43%, y_2 = 4.53%, F_1 = 6.20%, and F_2 = 6.46%. The close linear trend confirms the reliability of the model.

3. RESULTS

3.1 Single Ogee Sill Stilling Basin

Observations were made at single ogee sill heights (Z) of 10, 8, and 6 cm. The hydraulic jump formed after the single sill is type B. A single ogee sill installed at 80 cm downstream of the spillway toe (Figure 4). Observed data on laboratory of single ogee sill is shown on Table 2.

(a) Series 1, Z=10 cm, Q=21 L/s

(b) Series 2, Z=8 cm, Q=21 L/s

(c) Series 3, Z=6 cm, Q=21 L/s

Figure 4: Experimental observation of the single ogee sill stilling basin

Table 2: Average values of hydraulic flow parameters in single ogee sill

Series	Z	L	y_1	y_2	y_j	L_j	$(E_0-E_2)/E_0$	(E_2/E_1)
	(cm)	(cm)	(cm)	(cm)	(cm)	(cm)	(%)	(%)
SS-1	10	80	2.06	20.40	18.34	272.86	81.14	59.94
SS-2	8	80	2.05	20.86	18.81	273.57	80.73	60.24
SS-3	6	80	1.93	20.30	18.37	279.14	81.22	52.89

Figure 5 represents regression results of L_j, y_1, y_2, and Figure 6 represents the regression among dimensionless parameters for all single ogee sill stilling basin. The variables influencing the jump can be expressed as $f(y_1, y_2, y_c, v_1, v_2, q, L_j, y_j, Z, g) = 0$. Following Buckingham's π- theoretical of dimensional analysis and by taking y_1 and g to be repeated variables, it is possible to derive a dimensionless functional relation based on the observed data in the laboratory.

Regression lines were fitted to each scatter plot using power law relationships, and the goodness of fit (R^2) indicates correlation between hydraulic variables.

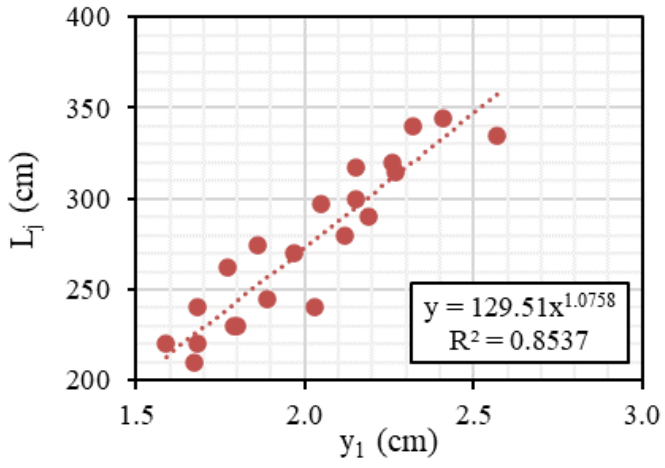

(a) Scatter plot of L_j vs y_1

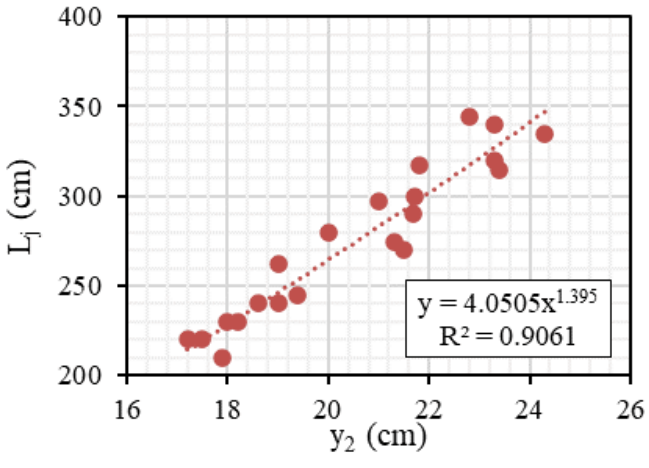

(b) Scatter plot of L_j vs y_2

Figure 5: Relationship between L_j, y_1 and y_2 of single ogee sill stilling basin

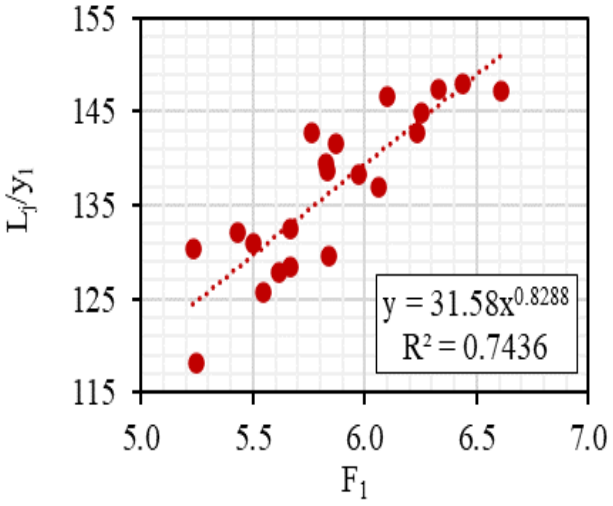

(a) Scatter plot of L_j/y_1 and F_1

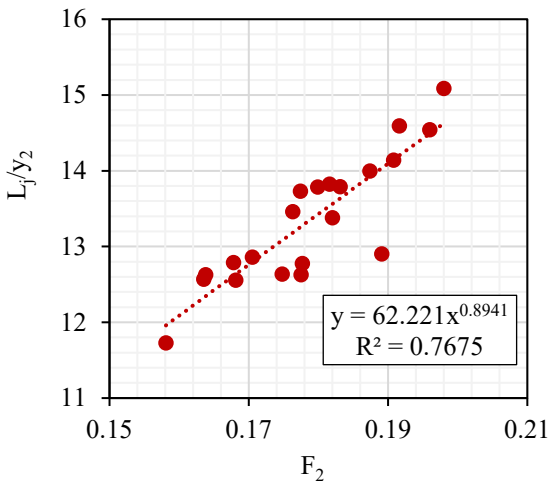

(b) Scatter plot of L_j/y_2 and F_2

Figure 6: The relationship between dimensionless parameters on single ogee sill stilling basin

Figure 5 presents that in both cases, L_j exhibits a strong positive nonlinear relationship, with higher goodness of fit for y_2 (R^2=0.9061) compared to y_1 (R^2=0.8537), suggesting that y_2 is a more reliable predictor of L_j. Figure 6 shows both plots exhibit positive power law trends, with moderate to strong correlations. The relationship between (L_j/y_2) and F_2 (R^2=0.7675) shows a slightly better fit than (L_j/y_1) and F_1 (R^2=0.7436), indicating that downstream flow conditions provide a marginally improved prediction of normalized jump length.

To evaluate hydraulic flow performance of sill stilling basin, a scoring method was employed based on ranking, that ranking and score are equal. The optimal series is the lowest cumulative score. The optimal hydraulic performance is the highest y_1 (decreasing F_1), the lowest y_2 and y_j (reducing height of sidewall), the shortest L_j (basin requirement), the largest relative energy loss $(E_0-E_2)/E_0$, and the smallest ratio of energy before and after hydraulic jump (E_2/E_1) as shown in Table 3. A lower value of (E_2/E_1) is considered better because it indicates more effective energy dissipation within the system. It means that a larger portion of the incoming energy has been dissipated. This is desirable in hydraulic engineering, as excess residual energy can lead to downstream issues such as bed erosion, structural damage, and flow instability. Therefore, a smaller (E_2/E_1) value reflects a more efficient system that better protects downstream areas by minimizing the energy carried by the flow.

Table 3: Assessment of hydraulic flow performance in single ogee sill stilling basin

Series	Scores						
	y_1	y_2	y_j	L_j	$(E_0-E_2)/E_0$	(E_2/E_1)	Cumulative
SS-1	1	2	1	1	2	2	9(1)
SS-2	2	3	3	2	3	3	16(3)
SS-3	3	1	2	3	1	1	11(2)

Note: the number in parentheses indicates ranking

Based on Table 3, the Series SS-1 model provides the optimal results, L = 80 cm, Z = 10 cm, produces the highest y_1, lowest y_j, and shortest L_j.

3.2 Double sill stilling basin (ogee and trapezoidal prism)

The double sill is combination of ogee sill (Z_1) and a trapezoidal prism sill (Z_2). The variation sill distances are L_2=0.5L_1 and L_2=0.25L_1. The sill height ratio is: Z_2=0.75Z_1 and Z_2=0.5Z_1. The flow rate was also seven flow rates (Figure 7). Observed data on laboratory of double sill stilling basin is shown on Table 4. The variables influencing the jump were expressed as $f(y_c, y_1, y_2, v_1, v_2, q, L_1, L_2, Z_1, Z_2, L_j, y_j, g) = 0$, and the repeated variables were y_1 and g.

(a) Series DS-1, Q = 17 L/s

(b) Series DS-2, Q = 17 L/s

(c) Series DS-3, Q = 17 L/s

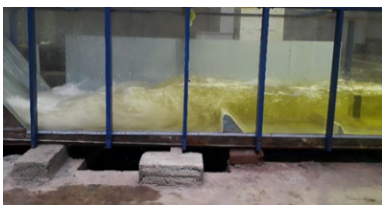

(d) Series DS-4, Q = 17 L/s

(e) Series DS-5, Q = 17 L/s

(f) Series DS-6, Q = 17 L/s

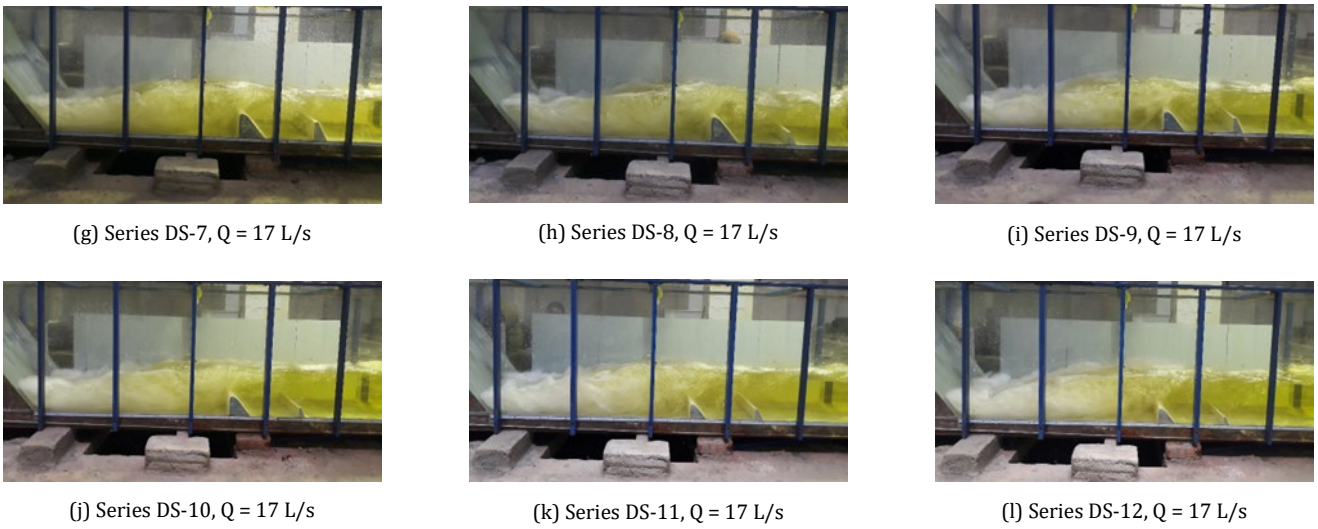

(g) Series DS-7, Q = 17 L/s (h) Series DS-8, Q = 17 L/s (i) Series DS-9, Q = 17 L/s

(j) Series DS-10, Q = 17 L/s (k) Series DS-11, Q = 17 L/s (l) Series DS-12, Q = 17 L/s

Figure 7: Observation on various configurations of the double sill stilling basin model

Table 4: Average values of hydraulic flow parameters in double sill stilling basin

Series	L_1	L_2	Z_1	Z_2	L_2/L_1	Z_2/Z_1	y_1	y_2	y_j	L_j	$(E_0-E_2)/E_0$	(E_2/E_1)
	(cm)	(cm)	(cm)	(cm)			(cm)	(cm)	(cm)	(cm)	(%)	(%)
DS-1	80	40	10	7.50	0.50	0.75	2.06	20.01	17.96	264.29	81.47	58.89
DS-2	80	40	10	5.00	0.50	0.50	2.05	20.26	18.21	255.00	81.26	58.65
DS-3	80	40	8	6.00	0.50	0.75	1.93	20.14	18.21	250.00	81.36	52.42
DS-4	80	40	8	4.00	0.50	0.50	2.01	20.26	18.25	257.00	81.26	56.56
DS-5	80	40	6	4.50	0.50	0.75	1.90	20.07	18.17	295.14	81.42	51.31
DS-6	80	40	6	3.00	0.50	0.50	1.91	21.14	19.23	282.29	80.47	53.88
DS-7	80	20	10	7.50	0.25	0.75	2.08	20.14	18.06	245.71	81.36	60.69
DS-8	80	20	10	5.00	0.25	0.50	2.20	20.23	18.03	247.14	81.28	67.36
DS-9	80	20	8	6.00	0.25	0.75	2.12	19.94	17.83	255.86	81.54	61.34
DS-10	80	20	8	4.00	0.25	0.50	2.02	20.09	18.07	256.86	81.41	57.14
DS-11	80	20	6	4.50	0.25	0.75	2.05	20.26	18.21	285.57	81.25	58.24
DS-12	80	20	6	3.00	0.25	0.50	1.99	20.07	18.08	287.57	81.42	56.08

Figure 8 shows the relationship between hydraulic jump length (L_j) and: (a) y_2; (b) (y_j=y_2-y_1), on all configurations of double sill stilling basin. L_j exhibits a positive nonlinear relationship with the independent variables, characterized by similar scaling exponent (~1.12). The coefficients of determination (R^2=0.601 for y_2 and R^2=0.5983 for y_j) indicate moderate correlation, suggesting comparable predictive capability of y_2 and y_j for estimating L_j.

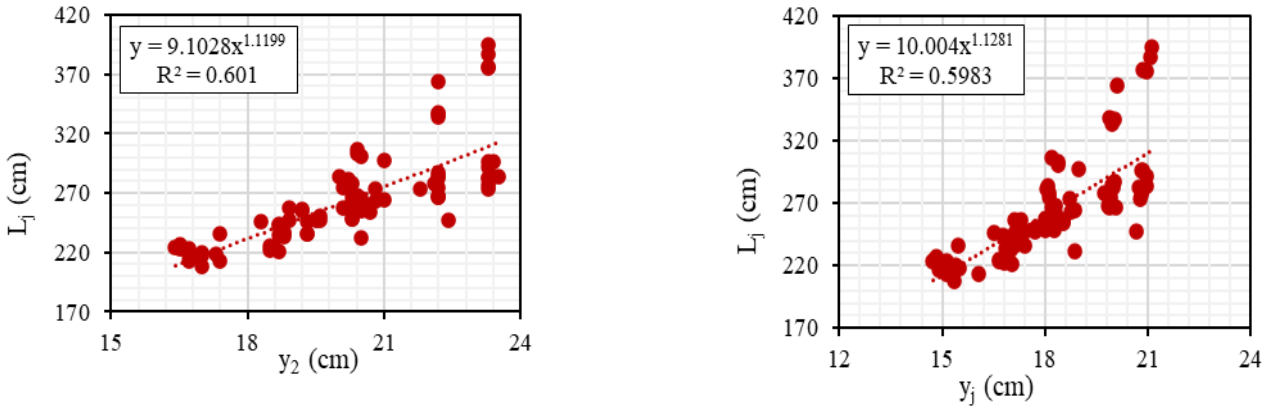

(a) Scatter plot of L_j vs y_2 (b) Scatter plot of L_j vs y_j

Figure 8: Relationship L_j with y_2 and y_j across double sill stilling basin configurations

The power law regression fits in Figure 9 indicates that (y_2/y_1) and (y_j/y_1) increase with F_1 with similar scaling exponents (~0.72-0.79) and moderate correlation (R^2≈0.66). (L_j/y_1) shows a weaker positive relationship (R^2=0.5134), while (E_2/E_1) exhibits a strong inverse trend with F_1 (R^2=0.8682), indicating significant energy dissipation as F_1 increases.

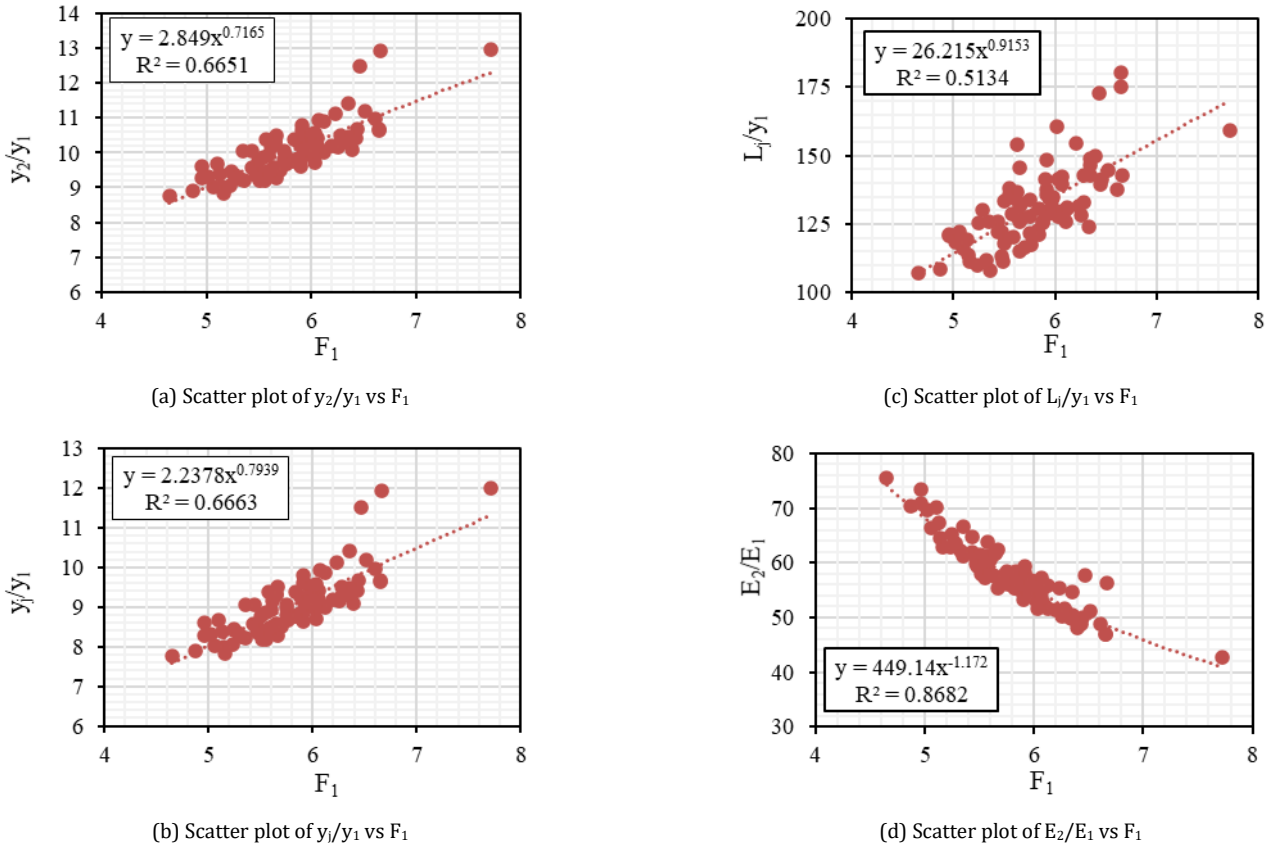

(a) Scatter plot of y_2/y_1 vs F_1

(c) Scatter plot of L_j/y_1 vs F_1

(b) Scatter plot of y_j/y_1 vs F_1

(d) Scatter plot of E_2/E_1 vs F_1

Figure 9: Dimensionless parameters relationship across double sill stilling basin configurations

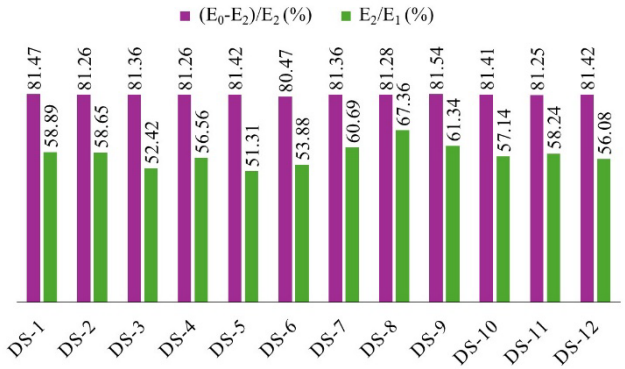

Figure 10: Comparison of energy dissipation characteristics across double sill configurations

The variation in energy dissipation parameters across double sill configurations is shown in Figure 10. The relative energy loss, $((E_0-E_2)/E_0)$, remains fairly consistent, staying within narrow range of about 80-82% for all configurations. This suggests that the total energy dissipation is not significantly affected by changes in the sill configuration. In contrast, the ratio (E_2/E_1) shows more variation, ranging from 51% to 67%. This indicates that the system depends on the specific configuration. DS-8 exhibits relatively higher (E_2/E_1) values, meaning less energy is dissipated between sections, whereas DS-5 shows lower values, pointing to more effective localized dissipation. This result suggests that changes in geometry mainly influence how energy is redistributed within the system rather than the total amount of energy dissipated.

The regression analysis shows that hydraulic variables have different levels of correlation. A strong relationship was found for energy efficiency ($R^2 \approx 0.87$), suggesting that this parameter can be predicted with relatively high reliability. In contrast, the jump length relationships and sequent depth relationships showed only moderate correlations ($R^2 \approx 0.51$-0.67), which indicates that other hydraulic processes, such as turbulence interaction and air entrainment, may also influence the observed behavior.

Scoring method on Table 5 is used to obtain the optimal hydraulic flow performance in the double sill stilling basin based on hydraulic flow performance in Table 4. Based on Table 5, Series DS-5 provides the optimal results, L_1 = 80 cm, Z_1 = 6 cm, L_2 = (0. $5L_1$) = 40 cm, Z_2 = ($0.75Z_1$) = 4.5 cm), produces the highest y_1 and lowest (E_2/E_1).

Table 5: Assessment of hydraulic flow performance in a double sill stilling basin

Series	Scores						
	y_1	y_2	y_j	L_j	$(E_0-E_2)/E_0$	(E_2/E_1)	Cumulative
DS-1	9	2	2	8	2	9	32(4)
DS-2	7	10	9	4	9	8	47(9)
DS-3	3	6	10	3	7	2	31(3)
DS-4	5	9	11	7	10	5	47(10)

Table 5: Assessment of hydraulic flow performance in a double sill stilling basin

Series	Scores						
	y_1	y_2	y_j	L_j	$(E_0-E_2)/E_0$	(E_2/E_1)	Cumulative
DS-5	1	3	7	12	3	1	27(1)
DS-6	2	12	12	9	12	3	50(11)
DS-7	10	7	4	1	6	10	38(7)
DS-8	12	8	3	2	8	12	45(8)
DS-9	11	1	1	5	1	11	30(2)
DS-10	6	5	5	6	5	6	33(5)
DS-11	8	11	8	10	11	7	55(12)
DS-12	4	4	6	11	4	4	33(6)

Note: The numbers in parentheses indicate ranking.

The regression of hydraulic variables relationship on Series DS-5 such as L_j, y_1, y_2, and y_j are represented in Figure 11.

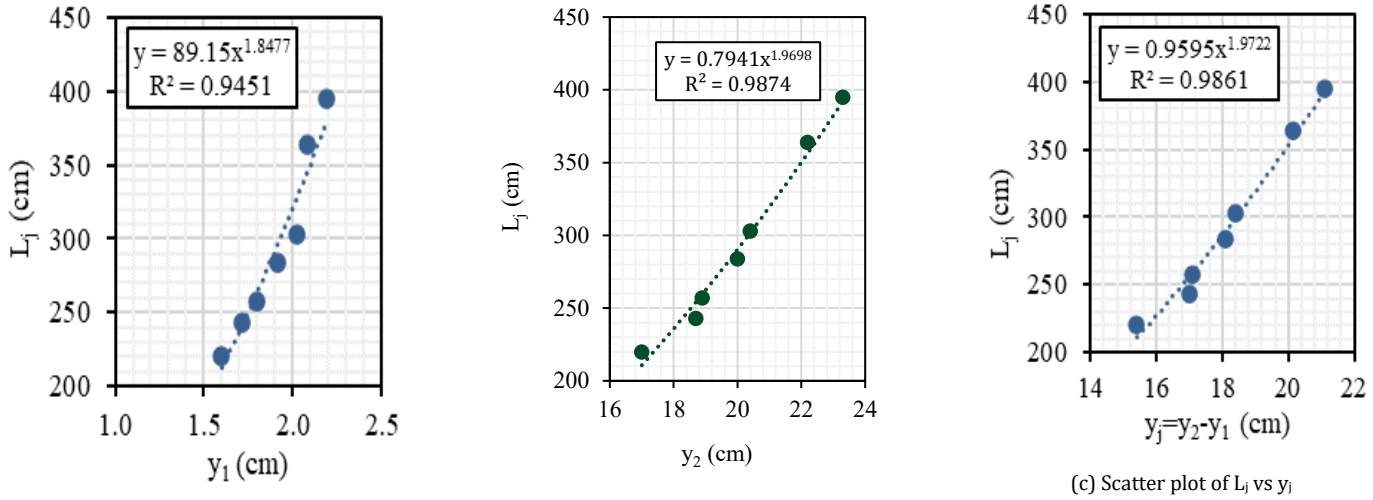

(a) Scatter plot of L_j vs y_1

(b) Scatter plot of L_j vs y_2

(c) Scatter plot of L_j vs y_j

Figure 11: Relationships among hydraulic variables in Series DS-5

The statistical relationships in Figure 11 demonstrate that in Series DS-5 the jump length (L_j) increases consistently with the hydraulic variables y_1, y_2, and y_j. The high R^2 values (≈0.94-0.99), indicate that these variables are strongly associated with the variation in jump length. Among them, y_2 gives the strongest relationship with L_j, suggesting that the sequent depth is the most reliable predictor of jump length.

The regression among dimensionless parameter relationship on Series DS-5 are represented in Figure 12. The dimensionless parameters relationships in Figure 12 further demonstrate that the hydraulic jump length parameters (L_j/y_1, L_j/y_2, L_j/y_j) exhibit increasing trends with the Froude number F_1, indicating that higher incoming flow intensity leads to a longer relative jump length. The corresponding regression equations provide strong fits to the experimental data, with high R^2 values (≈0.83-0.91). Whereas the energy ratios show decreasing trends with increasing Froude number F_1. This behavior indicates greater energy dissipation at higher flow intensities, confirming the effectiveness of the Series DS-5 configuration in reducing residual flow energy.

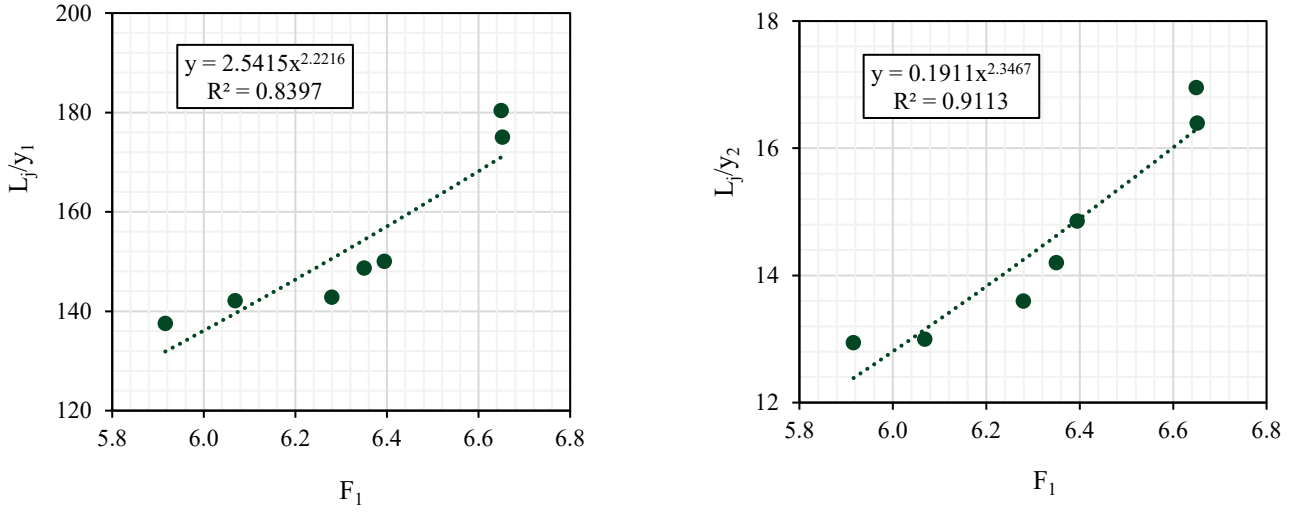

(a) Scatter plot of L_j/y_1 vs F_1

(b) Scatter plot of L_j/y_2 vs F_1

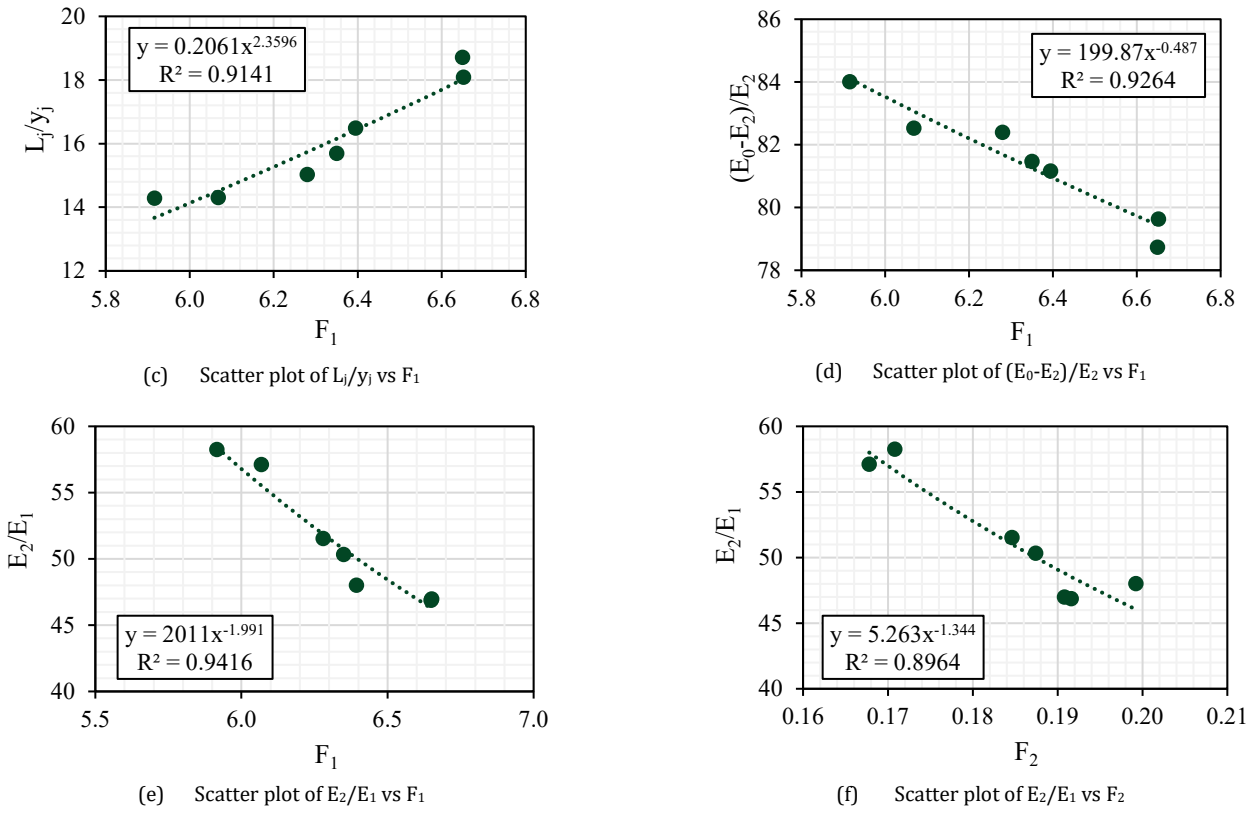

(c) Scatter plot of L_j/y_j vs F_1

(d) Scatter plot of $(E_0-E_2)/E_2$ vs F_1

(e) Scatter plot of E_2/E_1 vs F_1

(f) Scatter plot of E_2/E_1 vs F_2

Figure 12: Relationships among dimensionless parameters in Series DS-5

Table 6 presents the comparison of observed data on hydraulic models of horizontal apron, single ogee sill and double sill stilling basin. The compact stilling basin configuration (ogee and trapezoidal prism, DS-5) exhibits the highest overall energy dissipation ($(E_0-E_2)/E_0$) = 81.42%, while the single ogee sill (SS-1) shows a higher residual energy ratio (E_2/E_1) = 59.94%.

Table 6: Comparison of the optimal hydraulic flow parameter on each stilling basin

Type of Stilling Basin	Series	y_1 (cm)	y_2 (cm)	y_j (cm)	L_j (cm)	$(E_0-E_2)/E_0$ (%)	(E_2/E_1) (%)
Horizontal	0	1.31	21.27	19.97	254.29	80.36	25.85
Single Ogee Sill	SS-1	2.06	20.40	18.34	272.86	81.14	59.94
Ogee &Trapezoidal Prism	DS-5	1.90	20.07	18.17	295.14	81.42	51.31

Table 7 presents a comparative scoring analysis of the stilling basin configurations based on key hydraulic parameters within the Froude number range of $11<F_1<13.2$. Lower total scores indicate better overall performance, with the combination of ogee sill and trapezoidal prism sill configuration (DS-5) achieving the best ranking.

Table 7: Best of the optimal series performance scores

Type of Stilling Basin	Series	y_1	y_2	y_j	L_j	$(E_0-E_2)/E_0$	(E_2/E_1)	Scores
Horizontal	0	3	3	3	1	3	1	$14^{(3)}$
Single Ogee Sill	SS-1	1	2	2	2	2	3	$12^{(2)}$
Ogee & Trapezoidal Prism	DS-5	2	1	1	3	1	2	$10^{(1)}$

This ranking reflects the improved efficiency of the DS-5 configuration in balancing energy dissipation, flow characteristics, and geometric effectiveness. The results reinforce the advantage of incorporating additional structural elements to optimize hydraulic performance. The statistical diagrams show that the double sill configuration improves hydraulic performance than the single sill configurations. This suggests that the double sill arrangement creates a more stable and predictable flow behavior.

4. Discussion

Including statistical diagrams helps make the experimental results easier to interpret. Compared with tables alone, these graphs provide a clearer view of the trends, relationships, and variation within data. The regression plots also show that the proposed empirical equations are reliable and can be applied in engineering design, especially under strong hydraulic jump condition.

The experimental results clearly demonstrate that double sill configuration significantly enhances the hydraulic performance of stilling basin under strong hydraulic jump conditions. Excellent hydraulic parameters were shown in Series DS-5 with the best parameters in: y_2, y_j, and $((E_0-E_2)/E_2)$. The double sill configuration, an ogee sill (Z_1 = 6 cm) and a trapezoidal sill (Z_2 = 4.5 cm) placed at $0.5L_1$ downstream, offers superior hydraulic performance in energy dissipation, which produced the stable jumps, with kinetic energy conversion into turbulence. The placement of secondary sill downstream of the primary sill plays an important role in controlling the hydraulic jump. The flow experiences a two-stage energy dissipation mechanism: the first sill initiates flow deceleration and partial jump formation, while the second sill enhances turbulence, reinforces roller development, and stabilizes the jump location. This interaction leads to a more controlled and shorter hydraulic jump compared to single sill

stilling basin and horizontal apron stilling basin.

The findings reinforce the analytical framework of (Luo et al., 2021), who located hydraulic jump toe in sloped channels through sequent depth and jump length criteria. The regression-based approach in this study offers a simpler, non-iterate predictive tool of comparable accuracy, enhancing practical applicability. The series DS-5 configuration intensifies turbulence and roller formation, accelerating energy dissipation, and increases downstream depth, thereby mitigating local scour and uplift pressures. This improvement directly addresses failure mechanisms such as those observed in the Liu-Xi River sluice incident (Luo et al., 2021), where neglecting static jump effects compromised structural stability. Across sill-integrated stilling basin, geometry and placement critically influence flow behavior, pressure dynamics, and energy dissipation (Zhou et al., 2023). Bed roughness can reduce basin length by up to 50% while refinements in chute geometry and surface profiling further stabilize hydraulic jumps (Mohammed Saleh and Khassaf, 2023; Saleh and Khassaf, 2024; Fatimah et al., 2023; Macián-Pérez et al., 2020; Liu et al., 2020). Sill-induced turbulence, vortex generation, and air entrainment remain decisive in shaping flow structure and scour risk (Muhamad Bashar et al., 2025; Mahmoud and Mohamed, 2022; Zaffar and Hassan, 2023; Zhao et al., 2020). Double sill systems demonstrate superior performance under high Froude number flows, with calibrated sill height and spacing markedly improving dissipation efficiency and jump stability (Erryanto and Dermawan, 2024; Zhou et al., 2023; Mohammed Saleh and Khassaf, 2023). Numerical analyses confirm their adaptability under variable discharges while roughened beds further enhance turbulence control (Liu et al., 2020; Zaffar and Hassan, 2023). Their effectiveness in energy dissipation and downstream flow stability, indicating the need for continued refinement.

From an engineering standpoint, the enhanced performance of the double sill stilling basin offers significant implications for hydraulic structure design. Its capacity to shorten the hydraulic jump length while sustaining high energy dissipation efficiency enables the development of more compact stilling basins, thereby reducing construction costs and material demands. Moreover, the improvement in jump stability helps mitigate downstream scour and structural damage, ultimately strengthening the safety and long-term resilience of hydraulic systems.

5. Conclusion

This study aimed to evaluate the hydraulic performance of stilling basins with modified sill configurations. The experimental results demonstrated that the double sill configuration, an ogee sill (Z_1 = 6 cm) and a trapezoidal prism sill (Z_2 = 4.5 cm) spaced at $0.5L_1$ (40 cm), provided the optimal overall performance. This setup produced the lowest y_2 = 20.07 cm, the lowest y_j = 18.17 cm, and the highest energy loss ($(E_0–E_2)/E_0$ = 81.42%) along with the average energy dissipation efficiency (E_2/E_1 = 51.31%). Compared to both the horizontal and single sill basins, the Series DS-5 configuration offered superior hydraulic performance. The variation in sill height and spacing significantly influenced flow characteristics, with greater improvements observed in configurations that included a secondary sill placed closer to the primary ogee sill. This arrangement enhanced turbulence generation and stabilized the hydraulic jump effectively.

This study is among the first to experimentally evaluate combined ogee-trapezoidal sill configurations under strong hydraulic jump conditions. This research was conducted at the laboratory scale, under controlled flow conditions, and range of $11 < F_1 < 13.2$. The proposed configuration provides a practical design alternative for compact stilling basin design in high-energy hydraulic structures. Potential influences of scale effects, sediment transport processes, and air entrainment dynamics were not explicitly addressed. Consequently, further investigations are necessary to confirm the applicability of the proposed configuration at prototype scale and under more complex hydraulic environments.

Future research should also incorporate numerical modeling and sediment transport analyses to develop a more comprehensive understanding of flow and structure interactions in multi-sill systems.

References

Al-Fatlawi, T. J. M., Al-Mansori, N. J. H., and Othman, N. Y., 2020. Laboratory study of stilling basin using trapezoidal bed elements. Scientific Review Engineering and Environmental Studies (SREES), 29(4), Pp. 409–420. https://doi.org/10.22630/PNIKS.2020.29.4.35

Al-Mansori, N. J. H., Alfatlawi, T. J. M., Hashim, K. S., and Al-Zubaidi, L. S., 2020. The Effects of Different Shaped Baffle Blocks on the Energy Dissipation. Civil Engineering Journal, 6(5), Pp. 961–973. https://doi.org/10.28991/cej-2020-03091521

AlTalib, A. N., Mohammed, A. Y., and Hayawi, H. A., 2019. Hydraulic jump and energy dissipation downstream stepped weir. Flow Measurement and Instrumentation, 69, 101616. https://doi.org/10.1016/j.flowmeasinst.2019.101616

Benabid, S., Cherhabil, S., Ouakouak, A., and Bedjaoui, A., 2024. Characteristics of Hydraulic Jump in Asymmetrical Trapezoidal Channel With Rough Beds: Experimental Investigations. Studies in Engineering and Exact Sciences. https://doi.org/10.54021/seesv5n2-630

Chanson, H., 2022. Energy dissipation on stepped spillways and hydraulic challenges—Prototype and laboratory experiences. Journal of Hydrodynamics, 34(1), Pp. 52–62. https://doi.org/10.1007/s42241-022-0005-8

Dharmadhikari, P., and Gandhi, S., 2025. Investigation and Evaluation of Hydraulic Parameters of Stepped Spillway Based on ANN Models. Water Resources Management, 39(12), Pp. 6613–6632. https://doi.org/10.1007/s11269-025-04263-x

El-Saie, Y., Saleh, O., El-Sayed, M., Ali, A., and Sadek, E. E.-T. Y. M., 2023. Dissipation of Water Energy by Using a Special Stilling Basin Via Three-dimensional Numerical Model. The Open Civil Engineering Journal, 17(1). https://doi.org/10.2174/18741495-v17-230804-2022-78

Erryanto, S., and Dermawan, V., 2024. Double sill stilling basin to enhance energy dissipation for a strong hydraulic jump with a high Froude number. IOP Conference Series: Earth and Environmental Science, 1311(1). https://doi.org/10.1088/1755-1315/1311/1/012009

Fatimah, E., Azmeri, A., Aini, Q., Fauzi, M., and Rizalihadi, M., 2023. Analysis of the Hydraulic Jump Characteristics in a Stilling Basin to Avoid Dam Failure. International Journal of Disaster Management. https://doi.org/10.24815/ijdm.v6i1.31990

Hadi, H. A., and Al-Qaisi, A. Z., 2025. Behavior of the Alternative Types of USBR Basin with Changes in the Geometric Characteristics of the Straight Walls of the Stilling Basin. Engineering, Technology and Applied Science Research, 15(2), Pp. 20687–20692. https://doi.org/10.48084/etasr.9701

Idfi, G., Lasminto, U., and Kartika, A. A. G., 2024. Experimental Study of Energy Dissipation and Efficiency in a Stair-Shaped Modification of USBR Type III Stilling Basin. International Journal of Computational Methods and Experimental Measurements, 12(3), Pp. 237–250. https://doi.org/10.18280/ijcmem.120305

Jiang, L., Deng, Y., Liu, Y., Fang, L., and Guan, X., 2025. Insights into the Hydraulic Characteristics of Critical A-Jumps for Energy Dissipator Design. Water, 17(7), Pp. 960. https://doi.org/10.3390/w17070960

Kumar Jayant, H., and Jhamnani, B., 2024. Numerical study of submerged hydraulic jumps over triangular macroroughnesses. Journal of Hydroinformatics, 26(1), Pp. 51–71. https://doi.org/10.2166/hydro.2023.302

Kumcu, S. Y., and Ispir, K., 2022. Experimental and numerical modeling of various energy dissipater designs in chute channels. Applied Water Science, 12(12), Pp. 266. https://doi.org/10.1007/s13201-022-01792-3

Li, R., Splinter, K. D., and Felder, S., 2021. LIDAR Scanning as an Advanced Technology in Physical Hydraulic Modelling: The Stilling Basin Example. Remote Sensing, 13(18), Pp. 3599. https://doi.org/10.3390/rs13183599

Liu, Y., Zhang, D., Wu, J., Zhang, D., and Yang, M., 2020. Roughened Bed Stilling Basin and Its Hydraulic Jump Characteristics. Iop Conference Series Materials Science and Engineering. https://doi.org/10.1088/1757-899x/758/1/012082

Luo, G. Y., Cao, H., and Pan, H., 2021. Method to Locate the Toe of a Hydraulic Jump on Sloping Channels. KSCE Journal of Civil Engineering, 25(1), Pp. 124–139. https://doi.org/10.1007/s12205-020-0081-7

Macián-Pérez, J. F., Vallés-Morán, F. J., Sánchez-Gómez, S., De-Rossi-Estrada, M., and García-Bartual, R., 2020. Experimental Characterization of the Hydraulic Jump Profile and Velocity Distribution in a Stilling Basin Physical Model. Water. https://doi.org/10.3390/w12061758

Mahmoud, S., and Mohamed, R., 2022. The Effect of Unconventional Sills to Dissipate Energy Downstream Hydraulic Structures. Journal of Al-

Azhar University Engineering Sector. https://doi.org/10.21608/auej.2022.265706

Mohammed Saleh, L. A., and Khassaf, S. I., 2023. Effects of Chute Block Geometry on the Performance of the USBR II Stilling Basin. Jordan Journal of Civil Engineering. https://doi.org/10.14525/jjce.v17i3.12

Muhamad Bashar, N. A., Rozainy Zainol, M. R., Abdul Aziz, M. S., Ahmad Mazlan, A. Z., and Zawawi, M. H., 2025. Hydraulic Characteristics of Flow Over Dam Infrastructure: Preliminary Experimental Investigation. Iop Conference Series Earth and Environmental Science. https://doi.org/10.1088/1755-1315/1467/1/012025

Nasiri, K., Kavianpour, M. R., and Haghighi, S., 2012. The Baffle Blocks Effects of Pressure Characteristics on USBR III Basin Floor. Applied Mechanics and Materials, Pp. 212–213, 821–825. https://doi.org/10.4028/www.scientific.net/AMM.212-213.821

Rabiei, A., Mohammadzadeh-Habili, J., Chadee, A. A., Zomorodian, S. M., Jameel, M., and Azamathulla, H. M., 2023. Performance of a right-triangle stilling basin: a laboratory investigation. Water Supply, 23(9), Pp. 3912–3924. https://doi.org/10.2166/ws.2023.209

Raza, H., Sarwar, M. K., Haq, F. ul, Tariq, M. A. U. R., Altaf, T., and Abduljaleel, Y., 2023. Investigation of Hydraulic Performance of Standard and Modified USBR Type III Stilling Basin Using Scale Modeling: A Case Study of Mohmand Dam Spillway, Pakistan. Iranian Journal of Science and Technology, Transactions of Civil Engineering, 47(6), Pp. 4045–4057. https://doi.org/10.1007/s40996-023-01203-w

Roushangar, K., and Homayounfar, F., 2019. Prediction Characteristics of Free and Submerged Hydraulic Jumps on Horizontal and Sloping Beds using SVM Method. KSCE Journal of Civil Engineering, 23(11), Pp. 4696–4709. https://doi.org/10.1007/s12205-019-1070-6

Roy, D., Das, S., and Das, R., 2021. Characterisation of B type hydraulic jump by experimental simulation and numerical modeling using MacCormack technique. Modeling Earth Systems and Environment, 7(4), Pp. 2753–2768. https://doi.org/10.1007/s40808-020-01056-6

Saleh, L. A. M., and Khassaf, S. I., 2024. Evaluating the Hydraulic Performance of USBR II Stilling Basin with Rough Bed. Tikrit Journal of Engineering Sciences, 31(3), Pp. 93–104. https://doi.org/10.25130/tjes.31.3.9

Tajabadi, F., Jabbari, E., and Sarkardeh, H., 2018. Effect of the end sill angle on the hydrodynamic parameters of a stilling basin. The European Physical Journal Plus, 133(1), 10. https://doi.org/10.1140/epjp/i2018-11837-y

Tan, L., Deng, H., and Wang, J., 2025. Numerical Study on the Energy Dissipation Characteristics of Multi-Row Rectangular Damping Blocks in Spillway Stilling Basin, Pp. 785–792. https://doi.org/10.1007/978-3-031-90717-3_78

Zaffar, M. W., and Hassan, I., 2023. Hydraulic Investigation of Stilling Basins of the Barrage Before and After Remodelling Using FLOW-3D. Water Science & Technology Water Supply. https://doi.org/10.2166/ws.2023.032

Zaffar, M. W., Hassan, I., Latif, U. K., Jahan, S., and Ullah, Z., 2023. Numerical Investigation of Scour Downstream of Diversion Barrage for Different Stilling Basins at Flood Discharge. Sustainability. https://doi.org/10.3390/su151411032

Zhao, Z., Wang, J., and Zhu, D. Z., 2020. Energy Dissipation in a Deep Tailwater Stilling Basin With Partial Flaring Gate Piers. Canadian Journal of Civil Engineering. https://doi.org/10.1139/cjce-2018-0099

Zhou, Y., Wu, J., Zhao, H., Hu, J., and Bai, F., 2023. Hydraulic Performance of Wave-Type Flow at a Sill-Controlled Stilling Basin. Applied Sciences. https://doi.org/10.3390/app13085053